Model Predictive Control of DC-DC Converters to Mitigate the Effects of Pulsed Power Loads in Naval DC Microgrids

Mardani, Mohammad Mehdi; Khooban, Mohammad Hassan; Masoudian, Ali; Dragicevic, Tomislav

Published in:
I E E E Transactions on Industrial Electronics

DOI (link to publication from Publisher):
10.1109/TIE.2018.2877191

Publication date:
2019

Document Version
Accepted author manuscript, peer reviewed version

Model Predictive Control of DC-DC Converters to Mitigate the Effects of Pulsed Power Loads in Naval DC Microgrids

Mohammad Mehdi Mardani, Mohammad Hassan Khooban, *Senior Member, IEEE*, Ali Masoudian and Tomislav Dragičević, *Senior Member, IEEE*

***Abstract*—This paper proposes design of optimal and robust coordinated controller of hybrid energy storage system in a naval DC microgrid (MG) application. It is able to mitigate the negative effects of the pulsed power loads and meet the practical limitations of both converters input control and state variables signals based on IEEE standards. To do this, first, the dynamic model of the DC MG, which can represent in either all-electric aircraft or shipboard power systems is developed. Second, a novel model predictive controller (MPC) for energy storage converters is proposed such that all of the mentioned hard constraints are guaranteed. Third, a linear matrix inequality (LMI) approach is used to solve the MPC conditions. Finally, to evaluate the applicability and effectiveness of the proposed approach, some experimental tests are extracted. Obtained results verify better performance of the proposed approach over other state of the art control techniques.**

***Index Terms*—Pulsed power loads (PPLs), naval DC microgrid (MG), control of DC-DC converters, model predictive control (MPC).**

I. Introduction

RECENT developments in the electrification and power electronics technology have made all electric naval power systems (NPS) an attractive potential architecture for future applications. Among different architectures, DC microgrid type presents highly efficient and reliable power distribution that can be flexibly managed with simple control [1], [2]. Energy storage systems (ESS) play an important role to improve the reliability and efficiency of the DC microgrid. In the configuration of the NPSs, several types of loads such as pulsed power loads (PPLs), propulsion loads, ship service loads, and dedicated high power loads exist [3], [4]. Among them, the PPLs such as radars, sonars and electromagnetic weapons are loads that intermittently draw a large amount of power through a small period of time from the system. Due to the pulse behavior with high power characteristic of the PPLs, these kinds of loads present a very challenging issue for the operation of the system such as voltage deviation, voltage drop, tripping and even may result in a blackout the whole microgrid [5], [6].

The ESSs such as battery and supercapacitor (SC) storages are the essential interface to connect the PPLs to the grid. The battery energy storages are usually used in the DC microgrid with PPLs to compensate the requirements of the load in the critical conditions [7], [8]. Although the density of battery storages are relatively high, their volumetric power density is relatively low. The main ways to increase the power capacity of the batteries is to use multiple cells. However, the power-cost tradeoff and current sharing result in non-optimal battery storages [7]. Thus, battery storages are not capable to compensate the high power created by PPLs as primary power buffers. Due to the low internal resistance, high power density, and cycle life, the SCs have potential to solve the problem of battery storages. Although the energy density of SCs is less than battery storages, the power density of SCs is significantly larger than the battery storages [9]. In order to retain the high energy density beside the high power density, hybrid SCs-battery storages are used. In future NPS, the PPL is connected to the DC-link through the intermittent SCs. In PPL deactivation period, SCs are charged from the NPS with a smooth pattern, and disconnected when SCs are fully charged. During the PPL activation period, the SCs are rapidly discharged. Thus, in NPS with PPL, SCs are used as primary power buffers, while the batteries serve to smooth the SC charging procedures. For compensating the effects of PPLs, Ref. [8] indicates that the hybrid SCs-battery storages have better performance over the single battery storage. The analyses show that the hybrid storages decrease the internal losses, increase the discharging time and lifetime of the ESSs, simultaneously [10], [11].

Different kinds of hybrid configurations of the ESS for PPLs are presented in the literature. Connecting the SCs in parallel with the battery storages directly to the DC-link, which is well-known as a passive hybrid storage configuration [8]. The main advantages of the passive configuration are reducing the cost and power losses and easing the implementation. However, connecting the battery and SCs in a parallel configuration result in a limitation of power-sharing between them. Against the passive configuration, if the battery and SCs are connected to the DC link through the power electronic converters then the configuration is well known as an active hybrid one. Thus, based on the active configuration, the injected power to the DC-link can be regulated through converters. Refs. [12], [13] show that utilizing active hybrid storages configuration not only has a greater power capability but also the lower volume, weight, and current ripple of the ESSs can be guaranteed.

Since the ESSs are connected to the DC-link through the converters, the problem of controlling power electronic interfacing converters is a critical issue to analyze the stability and improve the efficiency of the microgrid system [12], [14]–[17]. Additionally, constructing a reliable control scheme plays an important role to govern the interaction between the PPLs and DC power system, and to mitigate the effect of the PPL in DC-link. Refs. [18], [19] present instantaneous power control (IPC) scheme for hybrid DC storages. The controller is equipped with hysteresis voltage protection on the DC bus. The structure of limit-based voltage control (LBVC) is presented in Refs. [18], [20]. The basic goal of the LBVC is to control the DC bus and charge the SC bank as fast as possible based on the limitations on the power of the converters and the available power of the sources. Refs. [12], [15], [19] study a continuous average current control (CACC) method to alleviate the effect of the pulse on the converters and storages. In the CACC technique, the output current of converters is tried to keep at the constant value. The CACC approach is suitable

This work was supported in part by the Office of Naval Research Global under the award number N62909-17-1-2106.

M. M. Mardani, M. H. Khooban, and T. Dragičević are with the Department of Energy Technology, Aalborg University, 9220 Aalborg East, Denmark. (e-mail: {mmm, kho, tdr}@ et.aau.dk).

Ali Masoudian is with the School of Electrical and Computer Engineering, Shiraz University, Shiraz 71847-64175, Iran (e-mail: alirad10120@gmail.com).

for the high PPLs cases, which result in a significant disturbance in the DC microgrid system. Ref. [21] presents an adaptive current–voltage control (ACVC) scheme. The basic concept of the ACDC is based on adaptive compensator proportional gain and the moving average measurement technique. In the ACDC approach, the current of the converter and voltage of the DC bus are controlled both together. However, Refs. [12], [15], [18]–[20] have some major drawbacks. First, the limitations on the current of the converters and voltage of the DC-link are only considered in the design procedure. The limitations on the current of the rectifier are not considered. Furthermore, to cope with the overcharging problem of the ESSs, it is necessary to consider the limitation for the voltages of the SCs and battery storages. Second, the control signal of the power converters needs to be inside a predefined region. This issue is not explicitly guaranteed based on the existing methods, but only indirectly, by inserting dedicated limiters within the control loops. Third, through the design procedure, the optimal solution must be obtained such that the hard constraint on the state variables and the control signal are guaranteed. However, the mentioned approaches have not addressed the problem of designing an optimal controller. The model predictive controller (MPC) provides a powerful framework to cope with the problem of applying hard constraints on the state and control variables and handling multivariable cases. Ref. [22] studies the problem of energy management for microgrid systems with renewable energy sources by utilizing an affine arithmetic method. Ref. [23] deployed an MPC approach to control linear induction machines. During recent years designing MPCs for power converters have been a promising control strategy in the literature [24]–[28]. The MPCs, which is widely employed in digital controllers, predict the suitable control signal for converters by minimizing a cost function [24]–[28]. According to the best knowledge of the authors, designing an optimal MPC controller for both battery and SC DC-DC converters to mitigate the effects of the PPLs has not been addressed in the literature, and this is the main contribution of this paper.

This paper designs a simple, robust, optimal, and efficient controller with hard constraints on the state and control signals of DC-DC converters. Straightforward dealing with such hard constraints is possible by utilizing the well-known MPC technique. Unlike the state of the art control methods, the developed procedure has benefits of controlling currents and voltages of the system as well as keeping the output voltages and currents of the microgrid in a small region around the operation point. Additionally, the SCs are recharged as fast as possible and the robust performance of the system against the PPL is assured. To do this, first, the state space model of the DC microgrid system is calculated analytically. Second, the MPC is proposed for DC microgrid systems with hybrid storages to track the constant reference signals and satisfy the mentioned hard constraints. The obtained MPC convex conditions cannot be solved analytically. Thus, the YALMIP LMI software in MATLAB is used to find the optimal solutions for the MPC problem. Finally, to evaluate the validity and applicability of the proposed approach, a laboratory scale DC microgrid is developed. By comparing the experimental results with the conventional energy management methods, the proposed control method can more effectively mitigate the effects of PPLs in the current of the converters, voltage of the DC link, and current of the grid.

Notations. The following notations are used throughout this paper. R, R^n, and $R^{n\times m}$ are the set of real values, n-dimensional vectors, and $n \times m$ matrices, respectively. The inequalities $M > 0$, $M < 0$, $M \geq 0$, and $M \leq 0$ for a symmetric matrix M mean that M is positive definite, negative definite, positive semi-definite, and negative semi-defenite, respectively. Additionally, the notation $diag\{N\}$ for a vector N is a diagonal matrix.

II. Hardware Description and Dynamic Modeling of The DC Microgrid System

This subsection investigates the hardware description and dynamical model of the DC microgrid in NPSs. As shown in Fig. 1, the DC microgrid usually consists of the land power interface, power generation, ESSs, loads, energy management control and system protection. The aim of each part is described as follows [3], [4]:

1. The land power interference is stepping up or down and converting the AC voltage to the level of the DC link through a rectifier unit.
2. The power generator, which generates the power from the fuel, is the main supplier part of the NPS.
3. The ESSs are usually used to compensate the fluctuations in the DC-link, which are obtained from step loads such as loss of a generator or PPLs.
4. The loads in NPS consist of a PPL, propulsion, ship service, and dedicated high power loads.
5. The energy management control system is a decentralized or centralized power management control, which communicates with the major loads and all of the sources. The goal of the control unit is to optimize the operation of the system according to some predetermined criteria.
6. The system protection is necessary to protect the AC and DC parts against faults. In DC NPSs, the protection is obtained by deploying the combination of converter control and other DC circuit breakers.

Fig. 1 illustrates the overall scheme of the DC microgrid system under study with PPL and hybrid storages. In Fig. 1, the ESSs are connected to the DC link by the concept of active hybrid configuration.

A. Hardware Description

As shown in Fig. 1, the main power supplier of the DC microgrid is the three-phase synchronous generator. The AC side is connected to the DC-link through the uncontrolled rectifier unit. Furthermore, the emulation of the voltage drop that appears in the DC-link is modeled by R_{MG} and L_{MG}.

The ESSs in the proposed DC microgrid is the SC and the battery bank, which are connected to the DC link through the buck and bidirectional buck-boost converters, respectively [29]. The battery bank can provide a longer-term support for the DC-link voltage in critical situations such as an island or highly loaded conditions. Additionally, the battery storage is charged in the normal conditions.

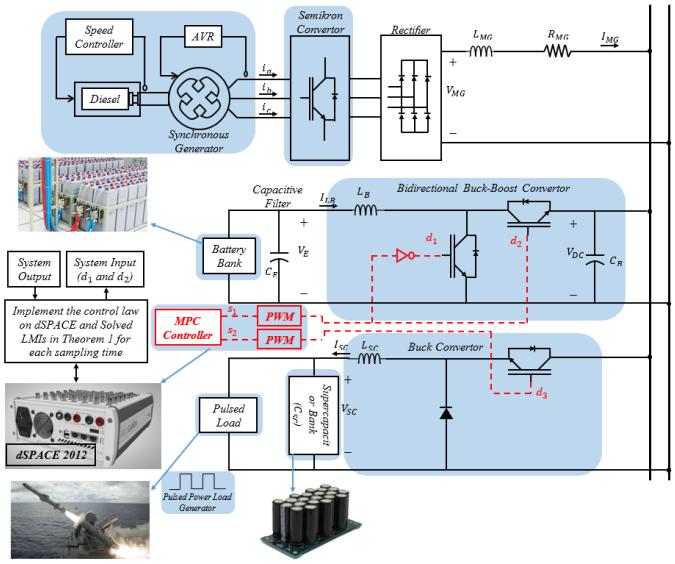

Fig. 1. The NPS case study.

This article has been accepted for publication in a future issue of this journal, but has not been fully edited. Content may change prior to final publication. Citation information: DOI 10.1109/TIE.2018.2877191, IEEE Transactions on Industrial Electronics

Furthermore, the PPLs of the NPS are connected to the DClink in pair with power buffers. In this paper, the intermittent power buffer takes the form of SC bank. The SC is first charged from the DC-link and then disconnected. Then, it gets rapidly discharged when the pulse is activated. In the following, the state space model of the DC microgrid system for the NPS is obtained.

The Delta Elektronika DC power supplies have been used to emulate batteries and SCs. In the following, the state space model of the DC microgrid system for the NPS is obtained.

B. Dynamic model of the ESS

In this paper, we consider the lithium-ion battery model, see Fig. 2(a) [30]–[32]. Over the state of the art battery models, the Thevenin model is one of the popular and appropriate ways to model a lithium-ion battery [30]–[32]. In Fig. 2 (a), R_p and C_p are the polarization resistance and capacitance, respectively. I_b is the load current. The state of charge (SoC) of the battery is defined as follows [30]–[32]:

$$SoC = SoC(0) - \frac{k_t}{C_{ESS}} \int I_b dt \tag{1}$$

where the nominal capacity of the battery is indicated by C_{ESS}. The time derivatives of equation (1) results in

$$\dot{SoC} = -\frac{k_t}{C_{ESS}} I_b = \frac{k_t}{R_b C_{ESS}} \left(V_p + V_{oc} - V_E\right) \tag{2}$$

Fig. 2 illustrates the overall model of the battery storage. By considering the average model of the bidirectional buck-boost converter and the Thevenin model of the lithium-ion battery (Fig. 2 (a)), the state space model of the ESS can be calculated as follows [32]:

$$\begin{cases} C_E \dfrac{dV_E}{dt} = \dfrac{V_P + V_{oc} - V_E}{R_b} - I_{LB} \\ C_P \dfrac{dV_P}{dt} = -\dfrac{V_P + V_{oc} - V_E}{R_b} - \dfrac{V_P}{R_P} \\ C_B \dfrac{dV_{DC}}{dt} = I_{LB} s_1 - I_{SC} s_2 + I_{MG} \\ L_B \dfrac{dI_{LB}}{dt} = V_E - V_{DC} s_1 - I_{LB} R_{LB} \end{cases} \tag{3}$$

where the V_E, V_P, V_{DC}, V_{oc} and I_{LB} are the ideal voltage source, Battery over-voltage, DC-link voltage, open-circuit voltage, and inductor current, respectively.

C. Dynamic model of PPL and DC voltage source

Fig. 3 shows the details for connecting the PPL to the DC-link. Whereas the PPL suddenly demands or rejects a very high power, the quick response ESS such as SC bank is vital to use. The PPL average dynamic model, is described via the following state space model [33]:

$$\begin{cases} C_{SC} \dfrac{dV_{C_{SC}}}{dt} = -\dfrac{PPL(t)}{V_{SC}} + I_{SC} \\ L_{SC} \dfrac{dI_{SC}}{dt} = -V_{SC} + V_{DC} s_2 - I_{SC} R_{SC} \end{cases} \tag{4}$$

D. Dynamic modeling of the main supplier of the DC grid

Fig. 4 illustrates the model and connection structure of the main supplier to the DC-link. Based on Fig. 4, the DC voltage source can be represented as follows:

$$L_{MG} \frac{dI_{MG}}{dt} = -I_{MG} R_{MG} + V_{MG} - V_{DC} \tag{5}$$

where the grid current is I_{MG}.

E. Overall state space model of a DC MG

Define $z = [z_1 \;\; z_2 \;\; z_3 \;\; z_4 \;\; z_5 \;\; z_6 \;\; z_7 \;\; z_8]^T = [V_E \;\; V_P \;\; V_{DC} \;\; I_{LB} \;\; V_{C_{SC}} \;\; I_{SC} \;\; I_{MG} \;\; SoC]^T \in R^7$. By considering the PPL as an unknown disturbance (i.e. $d(t) = PPL(t)$), the overall state space model of the DC MG in Fig. 1 can be calculated by utilizing equations (3), (4), and (5)

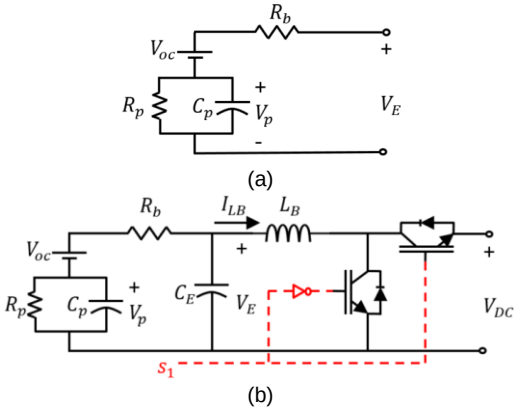

Fig. 2. The battery model. (a). Thevenin model of lithium-ion battery, (b). Connecting the battery to the grid.

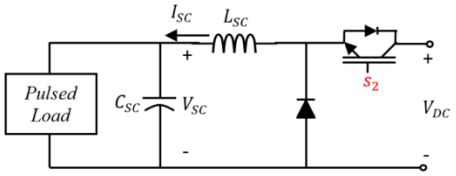

Fig. 3. The model of SC as an interface between the PPL and grid.

$$\begin{cases} \dot{z}_1 = \dfrac{z_2 + V_{oc} - z_1}{C_E R_b} - \dfrac{z_4}{C_E} \\ \dot{z}_2 = -\dfrac{z_2 + V_{oc} - z_1}{C_P R_b} - \dfrac{z_2}{C_P R_P} \\ \dot{z}_3 = \dfrac{1}{C_B} z_7 + \dfrac{1}{C_B} z_4 s_1 - \dfrac{1}{C_B} z_6 s_2 \\ \dot{z}_4 = \dfrac{1}{L_B} z_1 - \dfrac{1}{L_B} z_3 s_1 - \dfrac{R_{LB}}{L_B} Z_4 \\ \dot{z}_5 = \dfrac{1}{C_{SC}} z_6 - \dfrac{1}{C_{SC}} \dfrac{1}{z_5} d(t) \\ \dot{z}_6 = -\dfrac{1}{L_{SC}} z_5 + \dfrac{1}{L_{SC}} z_3 s_2 - \dfrac{R_{SC}}{L_{SC}} z_6 \\ \dot{z}_7 = -\dfrac{R_{MG}}{L_{MG}} z_7 + \dfrac{V_{MG}}{L_{MG}} - \dfrac{z_3}{L_{MG}} \\ \dot{z}_8 = \dfrac{-k_t}{R_b C_{ESS}} (z_2 + V_{oc} - z_1) \end{cases} \tag{6}$$

Employing the Jacobian linearization method [34]. The nonlinear system (6) can be linearized around the operating point $z^* = [z_1^* \;\; z_2^* \;\; z_3^* \;\; z_4^* \;\; z_5^* \;\; z_6^* \;\; z_7^* \;\; z_8^*]^T$, and $s = [s_1^* \;\; s_2^*] \in R^2$. One obtains

$$\begin{cases} \dot{x}(t) = \hat{A}x(t) + \hat{B}u(t) + \hat{D}d(t) \\ y(t) = Cx(t) \end{cases} \tag{7}$$

where $u(t) = s(t) - s^*(t)$, $x(t) = z(t) - z^*(t)$, $y(t)$, and $d(t)$ are the system input, state variables, output vectors, and disturbance input, respectively. $\hat{A} \in R^{8\times8}$, $\hat{B} \in R^{8\times2}$, $\hat{D} \in R^8$, and $C \in R^{5\times8}$ are known constant matrices

$$\hat{A} = \begin{bmatrix} -\frac{1}{C_E R_b} & \frac{1}{C_E R_b} & 0 & -\frac{1}{C_E} & 0 & 0 & 0 & 0 \\ \frac{1}{C_P R_b} & \hat{A}_{22} & 0 & 0 & 0 & 0 & 0 & 0 \\ 0 & 0 & 0 & \frac{1}{C_B} s_1^* & 0 & -\frac{1}{C_B} s_2^* & \frac{1}{C_B} & 0 \\ \frac{1}{L_B} & 0 & -\frac{1}{L_B} s_1^* & -\frac{R_{LB}}{L_B} & 0 & 0 & 0 & 0 \\ 0 & 0 & 0 & 0 & 0 & \frac{1}{C_{SC}} & 0 & 0 \\ 0 & 0 & \frac{1}{L_{SC}} s_2^* & 0 & -\frac{1}{L_{SC}} & -\frac{R_{SC}}{L_{SC}} & 0 & 0 \\ 0 & 0 & -\frac{1}{L_{MG}} & 0 & 0 & 0 & -\frac{R_{MG}}{L_{MG}} & 0 \\ \frac{k_t}{R_b C_{ESS}} & \frac{-k_t}{R_b C_{ESS}} & 0 & 0 & 0 & 0 & 0 & 0 \end{bmatrix},$$

This article has been accepted for publication in a future issue of this journal, but has not been fully edited. Content may change prior to final publication. Citation information: DOI 10.1109/TIE.2018.2877191, IEEE Transactions on Industrial Electronics

$$\hat{B}=\begin{bmatrix} 0 & 0 \\ 0 & 0 \\ \frac{1}{C_B}x_4^* & -\frac{1}{C_B}x_6^* \\ -\frac{1}{L_B}x_3^* & 0 \\ 0 & 0 \\ 0 & \frac{1}{L_{SC}}x_3^* \\ 0 & 0 \\ 0 & 0 \end{bmatrix}, \hat{D}=\begin{bmatrix} 0 \\ 0 \\ 0 \\ 0 \\ -\frac{1}{C_{SC}}\frac{1}{x_5^*} \\ 0 \\ 0 \\ 0 \end{bmatrix}, C=[0 \quad I^5 \quad 0]$$

where I^a and a are the identical matrix and its corresponding dimension, respectively. Additionally, $\hat{A}_{22}=-\frac{1}{C_P R_b}-\frac{1}{C_P R_P}$. Employing the Euler discretization technique. Consider T as a sampling time. Then, the continuous-time system (7) is converted to the following discrete model:

$$\begin{cases} x(k+1)=Ax(k)+Bu(k)+Dd(k) \\ y(k)=Cx(k) \end{cases} \tag{8}$$

where $A \in R^{n\times n}$, $B \in R^{n\times m}$, $C \in R^{q\times n}$, and $D \in R^{n\times p}$ are known constant system matrices with suitable dimension.

Remark 1. *One of the conventional and simple ways to cope with nonlinear systems is to linearize the nonlinear system around its operating point within each sampling period and then utilizing linear MPC approach. If the operating point of the nonlinear system is constant, then linearizing algorithm can be done only for one time. It must be noted that the linearized model is deployed for prediction algorithm, however the designed controller is applied to the nonlinear system [35].*

III. Practical Limitations

Fig. 1 shows the specific structure, which maximizes the performance and operation capability of the NPS even in the extremely critical conditions [3], [4]. Based on the guidelines of the IEEE recommendation for the DC electrical power system, the following limitations on the state variables are suggested to be considered through a design procedure [3], [4]. These constraints guarantee the quality of power and service for the NPS. All the devices in the DC NPS such as loads, storages, and generators are usually connected to the DC link through DC/DC, AC/DC, or DC/AC converters. Using the converters result in easing the connection of different size of ESSs, loads, and generator. Additionally, the fault currents will be limited by utilizing active configuration. The following limitations are extracted from IEEE standard for the DC power system [3], [4]:

1. In this paper, the AC grid is connected to the DC link by deploying uncontrolled rectifier unit. For the uncontrollable rectifiers, utilizing the semiconductor fuses or current limiting devices are necessary.
2. It needs to be ensured that the steady state voltage of the DC link remains within the tolerable bound [3], [4].
3. Due to the converters current limitation, some overcurrent type protections are necessary.
4. The voltage of the SCs must be set in a relatively constant and large value to compensate the effect of the high power of the PPL.
5. The converters are controlled by switching on-off signal controller, which is generated by pulse width modulator (PWM). The input signal of the PWM must be bounded between zero and one.

As shown in Fig. 1, in this paper, the uncontrolled rectifier current is illustrated by I_{MG}, which is the main supplier of the DC microgrid. The voltage of the DC link is denoted by V_{DC}. The converter currents are indicated by I_{LB} and I_{SC}. The SC voltage is described by V_{SC}. In the proposed approach, all of the mentioned hard constraints on the control signal and state variables are considered.

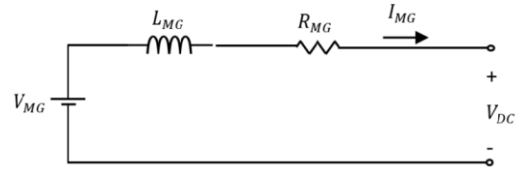

Fig. 4. Connecting the main supplier of the microgrid to the DC link.

IV. Constraint Model Predictive Controller

The MPC has been extensively used in industrial applications to solve the constrained control problems. The problem of designing an MPC is to solve a constraint optimization problem, which is obtained from an open-loop model with the sequence of control actions called control horizon [36]. In the MPC optimization problem, the evolutions of the state variables and control signal over a period of time named prediction horizon are computed. In each time instance, the constrained optimization problem is solved and only the first obtained control signal is implemented to the system. This kind of control is well-known as receding horizon control. Since the structure of the optimization problem in the MPC can be converted to the convex structure, the LMI approach can be used to numerically solve the constraint MPC conditions.

Remark 2. *The MPC method usually has several advantages over other existent control techniques. Some of them are described as follows [35]:*

1. *The multivariable cases and multi input multi output systems can be investigated through the MPC approach.*
2. *Hard constraints on the amplitude of the input and output signals can be considered.*
3. *The MPC approach can be deployed for controlling variety of processes, which are described by linear or nonlinear systems including delay, uncertainty and/or disturbances.*
4. *It is relatively easy to experimentally implement the MPC in real world applications.*

Next, the future output vectors are predicted and deployed in the optimization procedure. Consider the discrete-time system (8). Due to the absence of the exact value of disturbance, the disturbance is not considered through the design procedure. Based on (8), the prediction of the output variables among the horizon N can be calculated as follows:

$$y(k+N)=CA^N x(k)+\sum_{j=1}^{N} CA^{N-j}Bu(k+j-1) \tag{9}$$

Utilizing (9), one can conclude

$$Y(k)=Fx(k)+GU(k) \tag{10}$$

where

$$Y(k)=\begin{bmatrix} y(k+1) \\ y(k+2) \\ \vdots \\ y(k+N) \end{bmatrix}, U(k)=\begin{bmatrix} u(k) \\ u(k+1) \\ \vdots \\ u(k+N) \end{bmatrix},$$

$$F=\begin{bmatrix} CA \\ CA^2 \\ \vdots \\ CA^N \end{bmatrix}, G=\begin{bmatrix} CB & 0 & \cdots & 0 \\ CAB & CB & 0 & 0 \\ \vdots & \vdots & \ddots & \vdots \\ CA^{N-1}B & CA^{N-2}B & \cdots & CB \end{bmatrix},$$

In order to investigate the performance of the system, defining a mathematical expression as a performance index, or cost function is required. When the objective function is minimized, then it means that the system is operated in its desired conditions. One of the ways to predict the controller based on the MPC approach is to minimize the following objective function:

$$J=\big(Y(k)-w(k)\big)^T P\big(Y(k)-w(k)\big)+U^T(k)QU(k) \tag{11}$$

where P and Q are known positive matrices, which are the weighting matrices. The reference signal is denoted by $w(k)$. Minimizing the objective function (11) can be obtained by utilizing the following

This article has been accepted for publication in a future issue of this journal, but has not been fully edited. Content may change prior to final publication. Citation information: DOI 10.1109/TIE.2018.2877191, IEEE Transactions on Industrial Electronics

inequality:

Minimize γ such that:

$$\big(Y(k)-w(k)\big)^T P\big(Y(k)-w(k)\big)+U^T(k)QU(k)<\gamma \quad (12)$$

where the performance index γ is a positive definite function, which has to be minimized through the optimization problem [37]. The objective function (12) is not convex. In order to convert the condition (12) to the convex structure, the following fruitful lemma is deployed.

Lemma 1 (Schur complement) [38]***:*** *Consider an affine function F, which is partitioned as follows:*

$$F=\begin{bmatrix}F_{11} & F_{12}\\ F_{21} & F_{22}\end{bmatrix}$$

Then, $F<0$ is satisfied if and only if one of the following inequalities are satisfied:

$$\begin{cases}F_{11}<0\\ F_{22}-F_{21}F_{11}^{-1}F_{12}<0\end{cases} \text{ or } \begin{cases}F_{22}<0\\ F_{11}-F_{12}F_{22}^{-1}F_{21}<0\end{cases} \quad (13)$$

Theorem 1: *The objective function (12) is minimized if there exist any decision matrix variable $K(k)$ such that the following convex optimization problem with LMI constraints is satisfied:*

Minimize γ such that

$$\begin{bmatrix}H_{11}(k) & U^T(k)\\ U(k) & -(Q+G^TPG)\end{bmatrix}<0,\quad diag\{Fx(k)+GU(k)-Y_{max}\}<0, diag\{U-U_{max}\}<0,\quad diag\{Fx(k)+GU(k)-Y_{min}\}>0, diag\{U-U_{min}\}>0, \quad (14)$$

where

$$H_{11}(k)=\big(Fx(k)-w(k)\big)^T P\big(Fx(k)-w(k)\big)+U^T(k)G^TP\big(Fx(k)-w(k)\big)+\big(Fx(k)-w(k)\big)^T PGU(k)-\gamma.$$

$U(k)=K(k)x(k)$ and $u(k)\in R^m$ is obtained from the first m entries rows of matrix U. The obtained control signal not only tries to maintain the output variables at the constant value but also, minimize the performance index γ. Furthermore, some constraints on the amplitudes of the output and control signals are guaranteed to be inside a prechosen region, which is defined by U_{max}, U_{min}, Y_{max}, and Y_{min}.

Proof. Substituting (10) into (12), one has

$$\big(Fx(k)+GU(k)-w(k)\big)^T P\big(Fx(k)+GU(k)-w(k)\big)+U^T(k)QU(k)<\gamma \quad (15)$$

Eq. (15) can be rewritten in the following form:

$$\big(Fx(k)+GU(k)-w(k)\big)^T P\big(Fx(k)-w(k)\big)+\big(Fx(k)-w(k)\big)^T PGU(k)-\gamma+U^T(k)[Q+G^TPG]U(k)<0 \quad (16)$$

By employing Lemma 1, the bilinear matrix inequality (BMI) condition (16) is converted to the LMI ones as follows:

$$\begin{bmatrix}H_{11}(k) & U^T(k)\\ U(k) & -(Q+G^TPG)\end{bmatrix}<0 \quad (17)$$

where

$$H_{11}(k)=\big(Fx(k)-w(k)\big)^T P\big(Fx(k)-w(k)\big)+U^T(k)G^TP\big(Fx(k)-w(k)\big)+\big(Fx(k)-w(k)\big)^T PGU(k)-\gamma.$$

Additionally, the constraints on the amplitude of the output and control signals are considered as follows:

$$U(k)<U_{max}, U(k)>U_{min}, \quad Y(k)<Y_{max}, Y(k)>Y_{min}. \quad (18)$$

where $Y(k)=Fx(k)+GU(k)$. However, constraints (18) are not convex. In order to convert the non-convex conditions to the convex ones, representing the conditions (18) in a diagonal structure. Thus, the inequalities (18) are converted to the LMI and the proof is completed.

Remark 3. *More complicated types of MPC approaches such as the LPV-MPC or the nonlinear MPC, which have several advantages such as improving the accuracy of the model, are presented in the literature.*

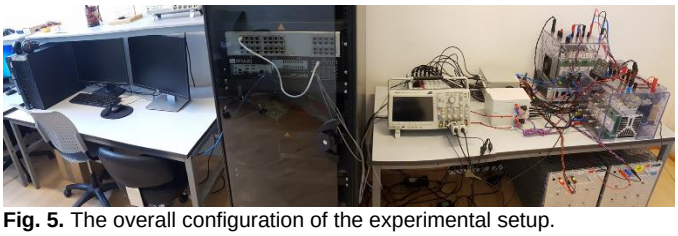

Fig. 5. The overall configuration of the experimental setup.

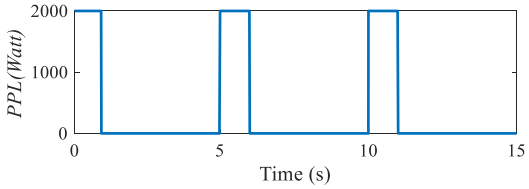

Fig. 6. The PPL signal.

These methods usually need to solve a typically non-convex, and large dynamic optimization problem, which require large amount of computational effort and time. We have to notice that form practical point of view, the computational speed is an essential issue. Apart from MPC approach, the control signals of the converters for the proposed DC microgrid need small sampling period and consequently high computation speed [39]. However, in linear MPC approaches, the optimal control problem can be presented in a convex quadratic programming structure and then solved through the quadratic programming solvers. One can conclude that the linear MPC, which is well-known for its outstanding speeds, construct a simple and compatible structure for controlling the proposed DC microgrid system [40].

Remark 4. *This paper proposes a simple, robust, systematic and effective approach to mitigate the destructive effects of the PPL. The PPL has a challenging effect on the NPSs. By reviewing the literature, one can conclude that designing the suitable controller for the dynamic DC microgrid in the NPS in the presence of PPL is rarely studied. The main reason is that the DC microgrids with PPLs need to respect several constraints on the amplitude of output and input signals, which makes the design using standard linear control techniques not possible. This paper fills this knowledge gap by combining the MPC and LMI, thus deploying a control method, which brings about voltage drop as small as possible. Additionally, tracking the reference value is one of the other important issues. However, the existing results cannot assure the desired performance. To sum up, the main contributions of this paper can be classified as follows:*

1. *For the first time, the mathematical dynamic model of the NPS with PPLs is introduced.*
2. *Hard constraints on the amplitude of the signals such as the currents of the converters and rectifiers and the voltages of the SC and DC-link are explicitly taken into account.*
3. *Suitable control signal for PWM (i.e. 0<u(t)<1) is designed. In other word, hard constraints are introduced on the amplitude of the signal control.*
4. *Proposing an MPC for the DC microgrid NPSs such that both DC-DC converters (for SC and battery) are controlled simultaneously.*
5. *The suggested control method is experimentally implemented and examined for the DC microgrid system in NPSs.*

V. Experimental Results, and Comparison

In this section, the performance of the proposed MPC for NPSs is experimentally investigated and compared with the newly published papers on energy control methods. The overall configuration of the experimental setup is presented in Fig. 5. The constraint MPC, which includes reference tracking of the output variables, converter control,

This article has been accepted for publication in a future issue of this journal, but has not been fully edited. Content may change prior to final publication. Citation information: DOI 10.1109/TIE.2018.2877191, IEEE Transactions on Industrial Electronics

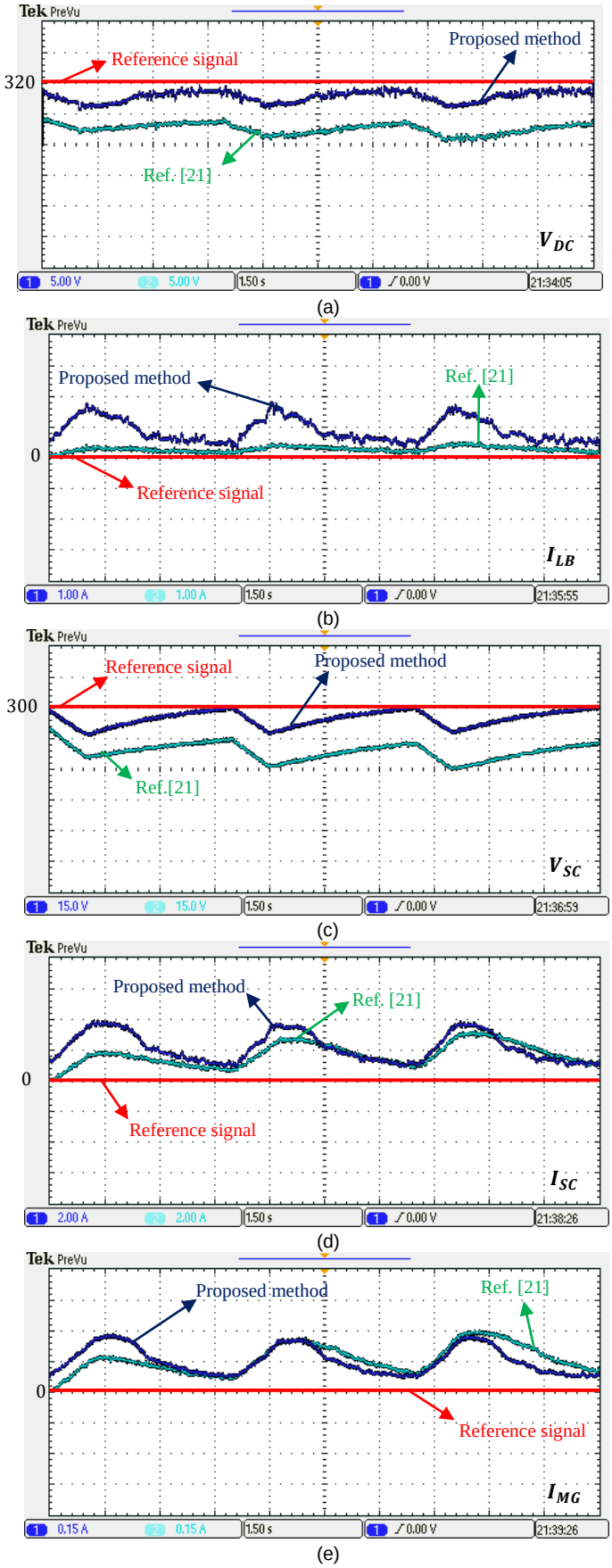

Fig. 7. The evolutions of the output variables. The blue (–), and green (–) colors illustrate the evolutions for the proposed approach and [21], respectively. The red color signal (–), which are drawn on top of images, are the reference signal.

constraints on the input and the output variables, and energy storage control, is simulated by MATLAB software. In this regard, a core i5, 2.7 GHz, 8 Gbytes RAM personal computer is employed. The hybrid DC microgrid system with single PPL, which is illustrated in Fig. 1, is implemented. Next, the MPC controller is applied to the DC microgrid system. The efficiency of the proposed approach is clearly indicated by comparing the results with the newly published control methods [15], [18]–[21]. In this experimental test, the PPL was a constant 2KW with the duty cycle and the frequency of the PPL are considered to be 20% and 0.2 Hz, respectively. The PPL signal is depicted in Fig. 6. The impedances R_{MG} and L_{MG} are considered to be 0.1Ω and $3mH$, respectively. In the SC side, the SC and inductor are considered to be $C_{SC} = 0.1F$, and $L_{SC} = 3\,mH$, respectively. Based on the selected parameter values, the experimental setup is designed and the effect of the PPL as a disturbance is investigated. In the battery side, the capacitor and the inductor are assumed to be, $L_B = 3mH$ and $C_B = 680\mu F$. Apart from the parameter values, the operating points and output references are considered to be

$$\begin{bmatrix} z_1^* \\ z_2^* \\ z_3^* \\ z_4^* \\ z_5^* \\ z_6^* \\ z_7^* \\ z_8^* \end{bmatrix} = \begin{bmatrix} V_E \\ V_p \\ V_{DC} \\ I_{LB} \\ V_{C_{SC}} \\ I_{SC} \\ I_{MG} \\ SoC \end{bmatrix} = \begin{bmatrix} 320 \\ 0 \\ 320 \\ 0 \\ 300 \\ 0 \\ 0 \\ 0.9 \end{bmatrix}, and \begin{bmatrix} V_{DC} \\ I_{LB} \\ V_{C_{SC}} \\ I_{SC} \\ I_{MG} \\ SoC \end{bmatrix} = \begin{bmatrix} 320 \\ 0 \\ 300 \\ 0 \\ 0 \\ 0.9 \end{bmatrix} \quad (19)$$

Which the output signals guarantee the following upper and lower bounds through the designing procedure:

$$\begin{bmatrix} V_{DC} \\ I_{LB} \\ V_{C_{SC}} \\ I_{SC} \\ I_{MG} \\ SoC \end{bmatrix}_{Upper\ bound} \leq \begin{bmatrix} 324 \\ 2 \\ 410 \\ 2 \\ 1 \\ 1 \end{bmatrix}, \text{and } \begin{bmatrix} V_{DC} \\ I_{LB} \\ V_{C_{SC}} \\ I_{SC} \\ I_{MG} \\ SoC \end{bmatrix}_{Lower\ bound} \geq \begin{bmatrix} 314 \\ -1 \\ 300 \\ -0.5 \\ -1 \\ 0.5 \end{bmatrix}$$

Then, apart from the mentioned constraint on the output signal, the constraint $0 \leq u(t) \leq 1$ on the amplitude of input signals is considered. The prediction horizon and the sampling period T in MPC are considered to be 4 and 1 ms, respectively. In addition, the weighting matrices P and Q in objective function (12) are defined such that 1) the state variables satisfy the dimensionless condition 2) the importance of each output variable is considered. Thus, matrices P and Q are considered to be:

$$P = I \otimes \begin{bmatrix} 320 & 0 & 0 & 0 & 0 \\ 0 & 1 & 0 & 0 & 0 \\ 0 & 0 & 320 & 0 & 0 \\ 0 & 0 & 0 & 1 & 0 \\ 0 & 0 & 0 & 0 & 100 \end{bmatrix}, Q = I \otimes \begin{bmatrix} 0.001 & 0 \\ 0 & 0.001 \end{bmatrix}$$

where $\otimes$ denotes the Kronecker product.

Now by applying the optimization algorithm presented in Theorem 1, the state feedback control gain matrices for each sampling period is calculated. The optimization problem is performed within YALMIP toolbox in Matlab environment [41]. Next, the control law is built with Matlab/Simulink software and experimentally implemented on the setup dSPACE 1202. The setup contains DS 1302 I/O board from dSPACE, Semikron Power Electronics Teaching Unit, and Micro Lab Box DS1202 PowerPC DualCore 2 GHz Processor board. Finally, the control signal is applied to the implemented DC microgrid system. The evolutions of the output variables based on the proposed MPC approach is illustrated in Fig. 7 with the blue lines.

Table 1. Two and infinity norms of error signal

	$\|y(t) - w(t)\|_2$	$\|y(t) - w(t)\|_\infty$
Proposed approach	44.10	688.63
The approach [21]	166.24	3528.5

In order to clearly indicate the better performance of the proposed approach, a comparison results with newly published control methods is presented. Thus, the authors use the control scheme presented in Ref. [21] adopted for the PPL system of this paper. Based on the control approach [21], the evolutions of the output variables are calculated and illustrated in Fig. 7 with the green lines. The DC link voltage is depicted in Fig. 7 (a). Based on the control method [21], the DC-link voltage is dropped. However, the proposed control method can compensate the effect of PPL and track the reference value of the DC-link voltage. Fig. 7 (b) illustrates the current of the bidirectional buck-boost converter. As can be seen from Fig. 7 (c), the SC is discharged and charge during pulsed on and off times, respectively. Based on the proposed control method, the SCs can charge as fast as possible. Furthermore, the voltage of the SC tracks the reference value. However, Ref. [21] cannot charge the SCs in the pulsed off times. Thus by increasing the time, the voltage of the SC reduced and the SC storage encountered with the over-discharging problem. This issue comes from the slow response of the approach [21]. The evolutions of the SC current is illustrated in Fig. 7 (d). Fig. 7 (e) illustrates the evolutions of the grid current. As can be seen, the generator must inject a larger amount of current to compensate the slow response of the [21]. As mentioned in the practical limitation part, this issue results in a destructive effect on the rectifier unit. However, the proposed approach holds the current of the rectifier in the predefined bounded.

Additionally, it is observed that both of the approaches can compensate the effect of the PPL. However, the proposed approach has several advantages in comparison with Ref. [21]. First, the transient response such as settling time of the proposed approach is significantly better. This issue results in charging the SCs as fast as possible. Second, in the steady-state conditions, the output variables are converged to the defined reference signals presented in (19). However, Ref. [21] cannot track the reference signal and the deviation is large. The two and the infinity norm of the error signal between output signals and their corresponding reference signals are investigated in Table 1. The remarkable improvement of the proposed MPC approach over the control method [21] is clearly shown in Table 1. Third, all of the limitations presented in Section III are considered through design procedure. Last but not least, the proposed control topology is designed such that both of the converters in Fig. 1 are controlled simultaneously.

Remark 5. *In the proposed approach, the load transient response is treated as a disturbance in the system [21]. As shown in Fig. 7, the transient response of the system during both pulse on and off times is significantly improved compared to the control approach [21]. The proposed controller suitably adjusts the converters such that the effects of the PPL disturbance is mitigated and the reference signals is suitably tracked during pulse on and off times, respectively. However, due to the slow transient response of the control approach [21], the error between output and reference signals are increased. Thus, one can conclude that the settling time of the proposed approach is less than the control approach [21].*

VI. Conclusions

As illustrated in experimental results, we can conclude that the effect of the PPL can be mitigated through the proposed energy management approach. The concept of the proposed energy management control is to control all the converters simultaneously by utilizing a multi-input-multi-output MPC approach. The input variables are the control signal of the converters and the output variables are the currents of the converters and rectifier, and the voltages of the DC link and SCs. According to the standards of the IEEE, there exist some limitations on the input and output variables. By utilizing the MPC technique, applying hard constraints on the control and output signals get possible. The MPC conditions are achieved in terms of LMI. Then by solving an LMI minimization problem, the optimal controller is obtained. By applying the controller to the DC microgrid system, we can conclude that both the transient and steady-state performance of the proposed approach is significantly better in comparison with the state of the art control methods.

References

[1] T. Dragičević, X. Lu, J. C. Vasquez, and J. M. Guerrero, "DC Microgrids Part I: A Review of Control Strategies and Stabilization Techniques," *IEEE Trans. Power Electron.*, vol. 31, no. 7, pp. 4876–4891, Jul. 2016.

[2] T. Dragičević, X. Lu, J. C. Vasquez, and J. M. Guerrero, "DC Microgrids Part II: A Review of Power Architectures, Applications, and Standardization Issues," *IEEE Trans. Power Electron.*, vol. 31, no. 5, pp. 3528–3549, May 2016.

[3] "IEEE Recommended Practice for 1 kV to 35 kV Medium-Voltage DC Power Systems on Ships," *IEEE Std 1709-2010*, pp. 1–54, Nov. ss2010.

[4] "IEEE Draft Recommended Practice for 1 kV to 35 kV Medium-Voltage DC Power Systems on Ships," *IEEE P1709D5 January 2018*, pp. 1–48, Jan. 2018.

[5] V. Salehi, B. Mirafzal, and O. Mohammed, "Pulse-load effects on ship power system stability," in *IECON 2010 - 36th Annual Conference on IEEE Industrial Electronics Society*, Glendale, AZ, USA, 2010, pp. 3353–3358.

[6] M. H. Khooban, T. Dragičević, F. Blaabjerg, and M. Delimar, "Shipboard Microgrids: A Novel Approach to Load Frequency Control," *IEEE Trans. Sustain. Energy*, vol. 9, no. 2, pp. 843–852, Apr. 2018.

[7] T. Ma, B. Serrano, and O. Mohammed, "Fuzzy logic based power and thermal management system design for multi-cell lithium-ion battery bank protection and operation," in *2014 Clemson University Power Systems Conference*, Clemson, SC, USA, 2014, pp. 1–5.

[8] R. A. Dougal, S. Liu, and R. E. White, "Power and life extension of battery-ultracapacitor hybrids," *IEEE Trans. Compon. Packag. Technol.*, vol. 25, no. 1, pp. 120–131, Mar. 2002.

[9] M. Ortuzar, J. Moreno, and J. Dixon, "Ultracapacitor-Based Auxiliary Energy System for an Electric Vehicle: Implementation and Evaluation," *IEEE Trans. Ind. Electron.*, vol. 54, no. 4, pp. 2147–2156, Aug. 2007.

[10] R. Lu, C. Zhu, L. Tian, and Q. Wang, "Super-Capacitor Stacks Management System With Dynamic Equalization Techniques," *IEEE Trans. Magn.*, vol. 43, no. 1, pp. 254–258, Jan. 2007.

[11] D. Linzen, S. Buller, E. Karden, and R. W. D. Doncker, "Analysis and evaluation of charge-balancing circuits on performance, reliability, and lifetime of supercapacitor systems," *IEEE Trans. Ind. Appl.*, vol. 41, no. 5, pp. 1135–1141, Sep. 2005.

[12] L. Gao, R. A. Dougal, and S. Liu, "Power enhancement of an actively controlled battery/ultracapacitor hybrid," *IEEE Trans. Power Electron.*, vol. 20, no. 1, pp. 236–243, Jan. 2005.

[13] P. Bajpai and V. Dash, "Hybrid renewable energy systems for power generation in stand-alone applications: A review," *Renew. Sustain. Energy Rev.*, vol. 16, no. 5, pp. 2926–2939, Jun. 2012.

[14] J. M. Carrasco *et al.*, "Power-Electronic Systems for the Grid Integration of Renewable Energy Sources: A Survey," *IEEE Trans. Ind. Electron.*, vol. 53, no. 4, pp. 1002–1016, Jun. 2006.

[15] D. Shin, Y. Kim, J. Seo, N. Chang, Y. Wang, and M. Pedram, "Battery-supercapacitor hybrid system for high-rate pulsed load applications," in *2011 Design, Automation Test in Europe*, Grenoble, France, 2011, pp. 1–4.

[16] F. Blaabjerg, Z. Chen, and S. B. Kjaer, "Power electronics as efficient interface in dispersed power generation systems," *IEEE Trans. Power Electron.*, vol. 19, no. 5, pp. 1184–1194, Sep. 2004.

[17] T. Dragičević, "Dynamic Stabilization of DC Microgrids with Predictive Control of Point of Load Converters," *IEEE Trans. Power Electron.*, pp. 1–1, 2018, doi. 10.1109/TPEL.2018.2801886.

[18] A. Mohamed, V. Salehi, and O. Mohammed, "Real-Time Energy Management Algorithm for Mitigation of Pulse Loads in Hybrid Microgrids," *IEEE Trans. Smart Grid*, vol. 3, no. 4, pp. 1911–1922, Dec. 2012.

[19] M. Farhadi and O. Mohammed, "Realtime operation and harmonic analysis of isolated and non-isolated hybrid DC microgrid," in *2013 IEEE Industry Applications Society Annual Meeting*, Lake Buena Vista, FL, USA, 2013, pp. 1–6.

[20] J. M. Crider and S. D. Sudhoff, "Reducing Impact of Pulsed Power Loads on Microgrid Power Systems," *IEEE Trans. Smart Grid*, vol. 1, no. 3, pp. 270–277, Nov. 2010.

[21] M. Farhadi and O. A. Mohammed, "Performance Enhancement of Actively Controlled Hybrid DC Microgrid Incorporating Pulsed Load," *IEEE Trans. Ind. Appl.*, vol. 51, no. 5, pp. 3570–3578, Apr. 2015.

[22] D. Romero-Quete and C. A. Cañizares, "An Affine Arithmetic-Based Energy Management System for Isolated Microgrids," *IEEE Trans. Smart Grid*, pp. 1–1, 2018, doi. 10.1109/TSG.2018.2816403.

[23] J. Zou, W. Xu, J. Zhu, and Y. Liu, "Low-Complexity Finite Control Set Model Predictive Control With Current Limit for Linear Induction Machines," *IEEE Trans. Ind. Electron.*, vol. 65, no. 12, pp. 9243–9254, Dec. 2018.

[24] T. Dragičević, M. Alhasheem, M. Lu, and F. Blaabjerg, "Improved model predictive control for high voltage quality in microgrid applications," in *2017 IEEE Energy Conversion Congress and Exposition (ECCE)*, Cincinnati, OH, USA, 2017, pp. 4475–4480.

[25] P. Karamanakos, T. Geyer, and S. Manias, "Direct Voltage Control of DC–DC Boost Converters Using Enumeration-Based Model Predictive Control," *IEEE Trans. Power Electron.*, vol. 29, no. 2, pp. 968–978, Feb. 2014.

[26] P. Karamanakos, T. Geyer, and S. Manias, "Direct Model Predictive Current Control Strategy of DC–DC Boost Converters," *IEEE J. Emerg. Sel. Top. Power Electron.*, vol. 1, no. 4, pp. 337–346, Dec. 2013.

[27] P. Karamanakos, G. Papafotiou, and S. Manias, "Model predictive control strategies for DC-DC boost voltage conversion," in *Proceedings of the 2011 14th European Conference on Power Electronics and Applications*, Birmingham, UK, 2011, pp. 1–9.

[28] T. Dragičević, "Model Predictive Control of Power Converters for Robust and Fast Operation of AC Microgrids," *IEEE Trans. Power Electron.*, vol. 33, no. 7, pp. 6304–6317, Jul. 2018.

[29] M. M. Mardani, N. Vafamand, M. H. Khooban, T. Dragičević, and F. Blaabjerg, "Design of Quadratic D-stable Fuzzy Controller for DC Microgrids with Multiple CPLs," *IEEE Trans. Ind. Electron.*, pp. 1–7, 2018.

[30] H.-W. He, R. Xiong, and Y.-H. Chang, "Dynamic Modeling and Simulation on a Hybrid Power System for Electric Vehicle Applications," *Energies*, vol. 3, no. 11, pp. 1821–1830, Nov. 2010.

[31] S. Lee, J. Kim, J. Lee, and B. H. Cho, "State-of-charge and capacity estimation of lithium-ion battery using a new open-circuit voltage versus state-of-charge," *J. Power Sources*, vol. 185, no. 2, pp. 1367–1373, Dec. 2008.

[32] L. Meng, T. Dragičević, and J. M. Guerrero, "Adaptive Control Design for Autonomous Operation of Multiple Energy Storage Systems in Power Smoothing Applications," *IEEE Trans. Ind. Electron.*, vol. 65, no. 8, pp. 6612–6624, Aug. 2018.

[33] D. K. Fulwani and S. Singh, *Mitigation of Negative Impedance Instabilities in DC Distribution Systems: A Sliding Mode Control Approach*. Springer Singapore, 2017.

[34] H. K. Khalil, "Nonlinear systems, 3rd," *New Jewsey Prentice Hall*, vol. 9, no. 4.2, 2002.

[35] E. F. Camacho and C. B. Alba, *Model Predictive Control*, 2nd ed. London: Springer-Verlag, 2007.

[36] H. S. Abbas, J. Hanema, R. Tóth, J. Mohammadpour, and N. Meskin, "An improved robust model predictive control for linear parameter-varying input-output models," *Int. J. Robust Nonlinear Control*, vol. 28, no. 3, pp. 859–880, Feb. 2018.

[37] E. F. Camacho and C. B. Alba, *Model Predictive Control*, 2nd ed. London: Springer-Verlag, 2007.

[38] C. Scherer and W. Siep, *Linear matrix inequalities in control*, vol. 3. Lecture Notes, Dutch Institute for Systems and Control, Delft, The Netherlands, 2000.

[39] J.-H. Lee and K.-B. Lee, "A Dead-Beat Control for Bridgeless Inverter Systems to Reduce the Distortion of Grid Current," *IEEE J. Emerg. Sel. Top. Power Electron.*, vol. 6, no. 1, pp. 151–164, Mar. 2018.

[40] R. Findeisen and F. Allgöwer, "An Introduction to Nonlinear Model Predictive Control," in *21st Benelux Meeting on Systems and Control, Veidhoven*, 2002, pp. 1–23.

[41] J. Lofberg, "YALMIP : a toolbox for modeling and optimization in MATLAB," in *2004 IEEE International Conference on Robotics and Automation (IEEE Cat. No.04CH37508)*, 2004, pp. 284–289.

[42] M. Novak, U. M. Nyman, T. Dragičević, and F. Blaabjerg, "Analytical Design and Performance Validation of Finite Set MPC Regulated Power Converters," *IEEE Trans. Ind. Electron.*, pp. 1–1, 2018 , doi. 10.1109/TIE.2018.2838073.

Mohammad Mehdi Mardani was born in Marvdasht, Fars, Iran. He received his M.Sc. degree from the Shiraz University of Technology (Iran) in 2014, where he is currently working toward the Ph.D. degree. Both in Control Engineering. Nowadays, he is a visiting Ph.D. student at Energy Technology Department, Aalborg University, Denmark. He is author or co-author of 12 conference papers and 12 journal papers. His current research interests include Takagi-Sugeno (TS) fuzzy control, LMI/SOS programming, model predictive control (MPC), power electronics and its application in power systems, advanced control of power electronic systems, and DC microgrid.

Mohammad-Hassan Khooban (M'13-SM'18) was born in Shiraz, Iran, in 1988. He received the Ph.D. degree from Shiraz University of Technology, Shiraz, Iran, in 2017. He was a research assistant with the University of Aalborg, Aalborg, Denmark from 2016 to 2017 conducting research on Microgrids and Marine Power Systems. Currently, he is a PostDoctoral Associate at Aalborg University, Denmark. His research interests include control theory and application, power electronics and its applications in power systems, industrial electronics, and renewable energy systems. He is author or co-author of more than 100 publications on journals and international conferences, plus one book chapter and one patent. He is currently serving as an Associate Editor of the Complexity Journal.

Ali Masoudian was born in Kazeroon, Fars, Iran, in 1987. He received the M.S. degree in power engineering from Shiraz University, Shiraz, Fars, Iran, in 2013. Currently, he is the Ph.D. student at Shiraz University and also with the Moheb Nirou consulting company as the head of power system studies and planning group. His research interest include power electronics, power system optimization and planning, micro grid design and management, shipboard power systems and electric vehicles control systems.

Tomislav Dragičević (S'09-M'13-SM'17) received the M.E.E. and the industrial Ph.D. degree from the Faculty of Electrical Engineering, Zagreb, Croatia, in 2009 and 2013, respectively. From 2013 until 2016 he has been a Postdoctoral research associate at Aalborg University, Denmark. From March 2016 he is an Associate Professor at Aalborg University, Denmark. His principal field of interest is overall system design of autonomous and grid connected DC and AC microgrids, and application of advanced modeling and control concepts to power electronic systems. He has authored and co-authored more than 120 technical papers in his domain of interest and is currently editing a book in the field. He serves as an Associate Editor in the IEEE TRANSACTIONS ON INDUSTRIAL ELECTRONICS and in the Journal of Power Electronics.